nature of the orbital in which the d-vacancy resides is best established experimentally by single-crystal EPR studies; such data are not currently available for **1**. However, EPR data are available for a mixed valence $(NH_3)_5Ru(pyrazine)Ru(NH_3)_5^{5+}$ ion ("Creutz-Taube ion"), which is crystallographically similar to **1** in that the pyrazine ring is staggered with respect to both $Ru(NH_3)_4$ units.[41] The unpaired electron mostly resides in an orbital perpendicular to the pyrazine plane, and delocalization over both Ru centers occurs via the $d(\pi)$ orbital on each Ru that participates in back-bonding with the pyrazine π^*-system. A recent combined EPR/MO study of Ru(III) complexes suggests that the half-occupied metal orbital tends to interact with a π-donor ligand.[42] This result implies that the Ru(III) d-vacancy in **1** (d_{xz}) is oriented so as to overlap favorably with the imidazole $p(\pi)$ system.

Concluding Remarks

The highly anisotropic lowest energy optical electron transfer absorption of **1** and the intimate electronic structural features of this chromophore have been characterized by the above spectroscopic and computational studies. These studies have quantified the intuitive expectation that the $d(\pi)/p(\pi)$ overlap between the Ru(III) d_{xz} orbital and the imidazole π-system must be strongly orientation dependent. In general, the same orbitals are involved in optical charge transfer (LMCT or MLCT) as in thermal electron transfer. Thus, an anisotropic optical electron transfer process implies that the rate of the corresponding thermal electron-transfer reaction should be sensitive to the orientation of the relevant donor/acceptor orbitals. The orientational dependence of long-range ("non-adiabatic") electron transfer on the electronic coupling between donor and acceptor orbitals is a topic of substantial current interest.[43-46] Our studies of **1** have the following implications for the use of $(NH_3)_5Ru^{III}$(his) as a probe of metalloprotein electron transfer: (1) The effective distance from a protein active site such as an Fe(II) heme to the probe should be that calculated to the *imidazole edge*. Owing to the strong electronic coupling between Ru(III) and the imidazole ligand, an electron transferred from the Fe(II) heme to the probe is "home free" once it reaches the imidazole edge. (2) The orientation of the $(NH_3)_5Ru^{III}$(his) unit relative to neighboring aromatic residues involved in electron-transfer pathways may strongly affect the rate of electron transfer.

Acknowledgment. The research of H.J.S. and J.A.P. was supported in part by the National Science Foundation (Grant CHE-8417548), the David and Johanna Busch Foundation, and the National Institutes of Health (the diffraction/crystallographic computing facility at Rutgers was purchased with Grant 1510 RRO 1486 O1A1). The research of K.K.-J. was supported by the National Institutes of Health (Grant GM-34111) and the donors of the Petroleum Research Fund, administered by the American Chemical Society. We thank Prof. S. Isied for a sample of the title complex and for helpful discussions. The computational studies benefited from electronic structure programs kindly supplied by Drs. M. Zerner and M. Krauss and from a grant of computer time from the Rutgers Center for Computer and Information Services.

Registry No. 1, 110528-80-8; $(NH_3)_5Ru$-imidazole^{3+}, 80593-52-8; $(NH_3)_5Ru$-4-methylimidazole^{3+}, 91209-01-7; $Ru(NH_3)_6^{3+}$, 18943-33-4; NH_3, 7664-41-7; imidazole, 288-32-4; 5-methylimidazole, 822-36-6.

Supplementary Material Available: Tables of hydrogen atom parameters and anisotropic thermal parameters (2 pages); listing of observed and calculated structure factors (7 pages). Ordering information is given on any current masthead page.

(41) Stebler, A.; Ammeter, J. H.; Furholz, U.; Ludi, A. *Inorg. Chem.* **1984**, *23*, 2764.
(42) Sakayi, S.; Yanase, Y.; Hagiwara, N.; Takeshita, T.; Naganuma, H.; Ohyoshi, A.; Ohkubo, K. *J. Phys. Chem.* **1982**, *86*, 1038.
(43) Siders, P.; Cave, R. J.; Marcus, R. A. *J. Chem. Phys.* **1984**, *81*, 5613.
(44) Ohta, K.; Closs, G. L.; Morokuma, K.; Green, N. J. *J. Am. Chem. Soc.* **1986**, *108*, 1319.
(45) Makinen, M. W.; Schichman, S. A.; Hill, S. C.; Gray, H. B. *Science* **1983**, *222*, 929.
(46) Closs, G. L.; Calcaterra, L. T.; Green, N. J.; Penfield, K. W.; Miller, J. R. *J. Phys. Chem.* **1986**, *90*, 3673.

Rhenium Carbonyl Semiquinone Complexes. Photochemical Addition of 9,10-Phenanthrenequinone to $Re_2(CO)_{10}$

Lynn A. deLearie and Cortlandt G. Pierpont*

Contribution from the Department of Chemistry and Biochemistry, University of Colorado, Boulder, Colorado 80309. *Received January 26, 1987*

Abstract: The photochemical reaction between $Re_2(CO)_{10}$ and 9,10-phenanthrenequinone has been investigated. In contrast with related reactions carried out with other quinones which gave tris(catecholate)rhenium(VI) products, the product obtained in this case is a binuclear rhenium(I) semiquinone carbonyl complex, $Re_2(CO)_7(PhenSQ)_2$. The complex crystallizes in the triclinic space group $P\bar{1}$ in a unit cell with dimensions $a = 9.509$ (2) Å, $b = 11.955$ (2) Å, $c = 15.131$ (4) Å, $\alpha = 74.36$ (2)°, $\beta = 87.20$ (2)°, $\gamma = 67.00$ (2)°, and $Z = 2$. The binuclear complex consists of $Re(CO)_4(PhenSQ)$ and $Re(CO)_3(PhenSQ)$ units linked by a bridge formed by one semiquinone oxygen of the chelated ligand of the $Re(CO)_4(PhenSQ)$ unit. This oxygen bridges to the vacant coordination site of the $Re(CO)_3(PhenSQ)$ unit. Strong intramolecular interactions between semiquinone ligands further stabilize the dimeric structure in the solid state. This compound is paramagnetic in solution but diamagnetic in the solid state due to magnetic coupling between semiquinone ligands. Electrochemistry shows both chemically reversible two-electron reduction and oxidation couples. Mechanistic implications for the formation of this dimer and the previously characterized tris-chelated rhenium(VI)–catecholate complexes, $Re^{VI}(3,5\text{-}DBCat)_3$ and $Re^{VI}(Cl_4Cat)_3$, are discussed.

The photochemistry of binuclear metal carbonyl complexes has been studied in the course of investigating routes to reactive metal complexes. Several reports have appeared on reactions of dimanganese and dirhenium decacarbonyl which describe either homolytic cleavage of the metal–metal bond to give the $M(CO)_5$ radical[1] or heterolytic displacement of a carbonyl ligand to give

0002-7863/87/1509-7031$01.50/0

the unsaturated $M_2(CO)_9$ species.[2] Stolzenberg and Muetterties have shown that ligand substitution reactions of $Re_2(CO)_{10}$ that are thermally initiated proceed exclusively by a carbonyl displacement mechanism. Photoinitiated reactions involve both CO displacement and Re–Re bond cleavage.[3] Evidence for the generation of transient radical complexes is often obtained by carrying out a secondary reaction to give products that are more easily characterized. Metal insertion into the C–Cl bond of a chlorocarbon has been used to study the photolytic formation of $Re(CO)_5$ by monitoring the appearance of $ReCl(CO)_5$ and an organic radical (eq 1).[4] Ortho- and paraquinones have also been

$$\cdot Re(CO)_5 + Ph_3CCl \rightarrow ClRe(CO)_5 + \cdot CPh_3 \quad (1)$$

used to trap the $M(CO)_5$ (M = Mn, Re) radicals (eq 2).[5] One-electron oxidation of the metal results in transfer of the

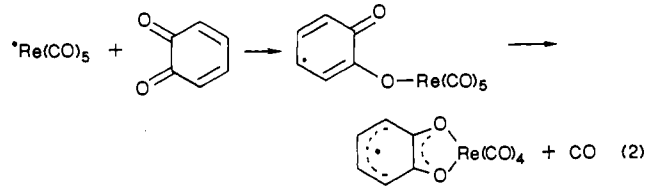

unpaired electron to the quinone ligand, giving a semiquinone product that can be characterized with EPR and conventional spectroscopic techniques. The transfer of electron spin density from an orbital localized on the metal to the quinone π orbital results in a significant change in the appearance of the EPR signal.[6]

The reaction between metal carbonyl complexes and *o*-benzoquinones provides a clean, efficient route to metal semiquinone and catecholate complexes.[7] Photolysis of a solution containing $Mn_2(CO)_{10}$ with excess 3,5-di-*tert*-butyl-1,2-benzoquinone leads to formation of tetrameric Mn(II) complex $[Mn(DBSQ)_2]_4$ containing semiquinone ligands,[8] while the same re-

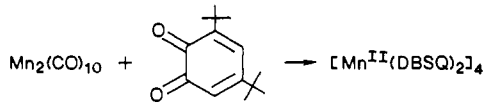

$$Re_2(CO)_{10} + DBBQ \rightarrow Re^{VI}(DBCat)_3$$

action carried out with $Re_2(CO)_{10}$ yields the Re(VI) catecholate complex $Re(DBCat)_3$.[9] Both reactions likely proceed through $M(CO)_n(DBSQ)$ complexes, formed as benzoquinone addition products to the photogenerated $M(CO)_5$ radicals. However, a tie between the carbonyl–semiquinone species and further reaction to give bis or tris quinone products has not been established. Reactions between $Re_2(CO)_{10}$ and benzoquinones proceed slowly, enabling study of the progressive addition of quinones to the metal with displacement of carbonyl ligands.

In marked contrast to the reactions between $Re_2(CO)_{10}$ and 3,5-di-*tert*-butyl-1,2-benzoquinone or tetrachloro-1,2-benzoquinone, which both product $Re^{VI}(Cat)_3$ products,[9] the related reaction carried out with 9,10-phenanthrenequinone produced a rhenium carbonyl semiquinone complex. In this report we describe details of the 9,10-phenanthrenequinone reaction and the details of further reactions which provide a link between the semiquinone–carbonyl complexes of rhenium and the tris(catecholate)rhenium(VI) products.

Experimental Section

$Re_2(CO)_{10}$ was obtained from Strem Chemical Co. and used as received. 9,10-Phenanthrenequinone, 3,5-di-*tert*-butyl-1,2-benzoquinone, and tetrachloro-1,2-benzoquinone were obtained from Aldrich Chemical Co. and used as received. All reactions were carried out in freshly distilled solvents with standard Schlenck line techniques. $Re(CO)_4$(DBSQ) and $Re(CO)_4(Cl_4SQ)$ were prepared photochemically by procedures similar to those used in earlier experiments.[5]

$Re_2(CO)_7(PhenSQ)_2$. 9,10-Phenanthrenequinone (0.33 g, 1.59 mmol) in 70 mL of toluene and 30 mL of methylene chloride was freeze–thaw–degassed for three cycles prior to addition to a similarly degassed solution of $Re_2(CO)_{10}$ (0.51 g, 0.79 mmol) in 40 mL of toluene. The resulting solution was photolyzed at room temperature for 24 h with use of a General Electric 275 watt sun lamp. The dark maroon, crystalline product was isolated from the solution after slow evaporation of the solvent and washed with cold toluene. $Re_2(CO)_7(PhenSQ)_2$ (0.21 g, 25% yield) was obtained by this procedure. Other materials obtained at the conclusion of the reaction were mainly unreacted starting compounds, and further photolysis could be used to form more $Re_2(CO)_7(PhenSQ)_2$.

$Re_2(CO)_7(PhenSQ)_2$ + DBBQ. 3,5-Di-*tert*-butyl-1,2-benzoquinone (0.18 g, 0.83 mmol) and $Re_2(CO)_7(PhenSQ)_2$ (0.14 g, 0.14 mmol) were heated at reflux in toluene for 24 h. Crystals of $Re(DBCat)_3$ formed from the solution and were characterized by EPR, UV–vis, and infrared spectroscopy.

Physical Measurements. Infrared spectra were recorded on a Beckman IR 4250 spectrometer and on an IBM IR/30 series FTIR spectrometer with samples prepared as KBr pellets or in methylene chloride solution in KBr sample cells. UV–vis spectra were recorded on a Hewlett Packard 8451A diode array spectrophotometer. Magnetic susceptibility measurements were made with use of the Faraday technique with a Sartorius 4433 microbalance. Electron paramagnetic resonance spectra were obtained on a Varian E-109 spectrometer with DPPH as the *g*-value standard. Cyclic voltammograms were obtained with a BAS-100 Electrochemical Analyzer. A platinum disc working electrode and a platinum wire counter electrode were used. The reference electrode was based on the Ag/Ag^+ couple and consisted of a silver acetate solution in contact with a silver wire placed in glass tubing with a Vycor frit at one and to allow ion transport. Tetrabutylammonium hexafluorophosphate was used as the supporting electrolyte and the ferrocene/ferrocenium couple was used as the internal standard, and values are reported relative to the Fc/Fc^+ couple.

Crystallographic Structure Determination on $Re_2(CO)_7(PhenSQ)_2$. The crystal was mounted on a glass fiber and aligned on a Nicolet P3F automated diffractometer. Axial and rotational photographs indicated triclinic symmetry for the crystal. Unit cell dimensions given in Table I were calculated from the centered positions of 25 intense reflections with 2θ values greater than 25°.

Positions of the Re atoms were determined from a three-dimensional Patterson map. Phases derived from the Re positions were used to locate all other non-hydrogen atoms of the structure. The final cycles of refinement converged with discrepency indices of $R = 0.043$ and $R_w = 0.043$. Maximum residual electron density of 1.80 $e^-/Å^3$ was observed in the vicinity of the Re atoms. Final positional and isotropic thermal parameters for all non-hydrogen atoms are listed in Table II. Tables containing anisotropic thermal parameters and structure factors are available as supplementary material.

Experimental Results

The $Re(CO)_4$(DBSQ) and $Re(CO)_4(Cl_4SQ)$ complexes were prepared by irradiation of toluene solutions containing $Re_2(CO)_{10}$ with the corresponding quinone and were identified by their characteristic EPR spectra. Similar mixtures in anisole solution

(1) (a) Wrighton, M.; Bredesen, D. *J. Organomet. Chem.* **1973**, *50*, C35. (b) Byers, B. H.; Brown, T. L. *J. Am. Chem. Soc.* **1975**, *97*, 947. (c) Kidd, D. R.; Brown, T. L. *J. Am. Chem. Soc.* **1978**, *100*, 4095. (d) Church, S. P.; Poliakoff, M.; Timney, J. A.; Turner, J. J. *J. Am. Chem. Soc.* **1981**, *103*, 7515. (e) Church, S. P.; Hermann, H.; Grevels, F.; Schaffer, K. *J. Chem. Soc., Chem. Commun.* **1984**, 785. (f) Seder, T. A.; Church, S. P.; Weitz, E. *J. Am. Chem. Soc.* **1986**, *108*, 7518.

(2) (a) Rothberg, L. J.; Cooper, N. J.; Peters, K. S.; Vaida, V. *J. Am. Chem. Soc.* **1982**, *104*, 3536. (b) Hepp, A. F.; Wrighton, M. S. *J. Am. Chem. Soc.* **1983**, *105*, 5934. (c) Herrick, R. S.; Brown, T. L. *Inorg. Chem.* **1984**, *23*, 4550.

(3) Stolzenberg, A. M.; Muetterties, E. L. *J. Am. Chem. Soc.* **1983**, *105*, 822.

(4) Wrighton, M. S.; Ginley, D. S. *J. Am. Chem. Soc.* **1975**, *97*, 2065.

(5) (a) Alberti, A.; Camaggi, C. M. *J. Organomet. Chem.* **1979**, *181*, 355. (b) Pasimeni, L.; Zanonato, P. L.; Corvaja, C. *Inorg. Chim. Acta* **1979**, *37*, 241. (c) Bowmaker, G. A.; Campbell, G. K. *Aust. J. Chem.* **1979**, *32*, 1897. (d) Abakumov, G. A.; Cherkasov, V. K.; Shalnova, K. G.; Teplova, I. A.; Razuvaev, G. A. *J. Organomet. Chem.* **1982**, *236*, 333. (e) Sarbasov, K.; Tumanskij, B. L.; Solodovnikov, S. P.; Bubnov, N. N.; Prokof'ev, A. I.; Kabachnik, M. I. *Izv. Akad. Nauk USSR* **1982**, 550. (f) Foster, T.; Chen, K. S.; Wan, J. K. S. *J. Organomet. Chem.* **1980**, *184*, 113. (g) Creber, K. A. M.; Wan, J. K. S. *J. Am. Chem. Soc.* **1981**, *103*, 2101. (h) Vlcek, A., Jr. *J. Organomet. Chem.* **1986**, *306*, 63.

(6) (a) Cass, M. E.; Greene, D. L.; Buchanan, R. M.; Pierpont, C. G. *J. Am. Chem. Soc.* **1983**, *105*, 2680. (b) Buchanan, R. M.; Wilson-Blumenberg, C.; Trapp, C.; Larsen, S. K.; Greene, D. L.; Pierpont, C. G. *Inorg. Chem.* **1986**, *25*, 3070.

(7) Pierpont, C. G.; Buchanan, R. M. *Coord. Chem. Rev.* **1981**, *38*, 45.

(8) Lynch, M. W.; Hendrickson, D. N.; Fitzgerald, B. J.; Pierpont, C. G. *J. Am. Chem. Soc.* **1984**, *106*, 2041.

(9) (a) deLearie, L. A.; Pierpont, C. G. *J. Am. Chem. Soc.* **1986**, *108*, 6393. (b) deLearie, L. A.; Haltiwanger, R. C.; Pierpont, C. G. *Inorg. Chem.* **1987**, *26*, 817.

Table I. Crystal Data and Details of the Structure Determination and Refinement for $Re_2(CO)_7(O_2C_{14}H_8)_2$

formula	$Re_2O_{11}C_{35}H_{16}$
mol wt	984.93
space group[a]	$P\bar{1}$
crystal system	triclinic
a (Å)[b]	9.509 (2)
b (Å)	11.955 (2)
c (Å)	15.131 (4)
α (deg)	74.36 (2)
β (deg)	87.20 (2)
γ (deg)	67.00 (2)
volume (Å^3)	1521.6 (6)
Z	2
d_{calcd} (g cm^{-3})	2.15
d_{exptl} (g cm^{-3})	2.10 (2)
$F(000)$	928
μ (cm^{-1})	84.66
crystal dimens (mm)	0.23 × 0.15 × 0.05
diffractometer	Nicolet P3F
data collected	$\pm h,\pm k,+l$
radiation (Å)	Mo Kα (0.71069)
monochromator angle (deg)	12.2
temp (K)	294–296
scan technique	θ–2θ
scan range (2θ), min – max	3.0–55.0
scan speed, (deg/min)	8.0–60.0
scan range	0.7° below Kα_1 and 0.7° above Kα_2
bkgd: stationary crystal – stationary counter bkgd time	0.5 (scan time)
unique reflcns measured	7050
obsd reflcns	3525
criterion	$F > 6(\sigma(F))$
absorption corr	empirical
transmission factors	0.964–0.544
programs used	SHELXTL[c]
scattering factors	neutral atoms[d]
R_1 and R_2[e]	0.0433, 0.0428
goodness of fit	1.120
weight	$1/(\sigma(F)^2 + 0.0003F^2)$
no. of parameters	433
ratio of observations to parameters	8.14
max shift/error (non-hydrogen)	0.011
residual electron density (e$^-$/Å^3)	1.80

[a] *International Tables for X-ray Crystallography*; Kynoch Press: Birmingham, England, 1965; Vol. 1. [b] Cell dimensions were determined by least-squares fit of the setting angles of 20 reflections with 2θ in the range 20–30°. [c] G. M. Sheldrick, SHELXTL, A Program for Crystal Structure Determination, Nicolet Instrument Corp., P.O. Box 4370, Madison, WI 53711-0508. [d] *International Tables for X-ray Crystallography*; Kynoch Press: Birmingham, England, 1974; Vol. 4, pp 55–60, 99–101, 149–150. [e] The quantity minimized in the least-squares procedures is $\sum w(|F_o| - |F_c|)^2$. $R_1 = \sum||F_o| - |F_c||/\sum|F_o|$. $R_2 = [\sum w(|F_o| - |F_c|)^2/\sum w(F_o)^2]^{1/2}$.

Table II. Atomic Coordinates (×10^4) and Temperature Factors (Å × 10^3) for $Re_2(CO)_7(O_2C_{14}H_8)_2$

	x	y	z	U[a]
Re(1)	2240 (1)	341 (1)	3605 (1)	33 (1)
Re(2)	−1011 (1)	1241 (1)	1740 (1)	36 (1)
O(1)	3607 (11)	−71 (9)	1745 (7)	64 (5)
O(2)	5559 (11)	−884 (10)	4351 (8)	70 (5)
O(3)	2336 (12)	−2346 (8)	4136 (7)	67 (5)
O(4)	1239 (11)	602 (9)	5580 (7)	59 (5)
O(5)	1128 (12)	−1514 (8)	2042 (7)	73 (5)
O(6)	−1883 (13)	1061 (10)	−96 (7)	77 (6)
O(7)	−3577 (13)	358 (11)	2404 (8)	86 (7)
O(8)	−202 (8)	1388 (7)	3104 (5)	36 (4)
O(9)	1899 (9)	2286 (7)	3259 (6)	39 (4)
O(10)	−2327 (9)	3196 (7)	1530 (5)	37 (4)
O(11)	605 (8)	2096 (7)	1377 (5)	35 (3)
C(1)	3044 (14)	125 (11)	2400 (9)	45 (6)
C(2)	4320 (14)	−419 (11)	4066 (9)	42 (6)
C(3)	2300 (14)	−1326 (10)	3935 (10)	42 (6)
C(4)	1558 (14)	527 (11)	4872 (10)	39 (6)
C(5)	323 (14)	−484 (11)	1952 (9)	43 (6)
C(6)	−1541 (16)	1116 (12)	620 (10)	51 (7)
C(7)	−2570 (16)	656 (14)	2164 (10)	54 (7)
C(8)	−669 (14)	2551 (11)	3230 (8)	39 (5)
C(9)	498 (14)	3003 (11)	3271 (8)	36 (5)
C(10)	11 (15)	4275 (11)	3374 (9)	41 (6)
C(11)	−1530 (17)	4927 (12)	3573 (10)	51 (7)
C(12)	−2605 (15)	4339 (12)	3651 (9)	48 (7)
C(13)	−2186 (14)	3160 (12)	3469 (8)	41 (6)
C(14)	1117 (16)	4797 (12)	3290 (10)	53 (7)
C(15)	643 (21)	6009 (14)	3381 (12)	79 (9)
C(16)	−878 (21)	6666 (13)	3591 (15)	101 (11)
C(17)	−1901 (19)	6128 (13)	3677 (11)	66 (8)
C(18)	−3259 (15)	2592 (13)	3533 (9)	48 (6)
C(19)	−4715 (16)	3183 (13)	3787 (10)	59 (7)
C(20)	−5125 (15)	4350 (15)	3982 (11)	69 (8)
C(21)	−4109 (17)	4913 (15)	3906 (10)	66 (8)
C(22)	−1530 (13)	3857 (11)	1463 (8)	34 (5)
C(23)	105 (13)	3271 (11)	1357 (8)	35 (5)
C(24)	1070 (13)	3978 (10)	1191 (9)	39 (5)
C(25)	361 (15)	5302 (12)	1070 (9)	48 (6)
C(26)	−1293 (15)	5922 (11)	1153 (9)	46 (6)
C(27)	−2216 (14)	5213 (11)	1365 (8)	37 (5)
C(28)	2612 (14)	3370 (12)	1155 (10)	48 (6)
C(29)	3525 (15)	4029 (14)	971 (11)	61 (7)
C(30)	2856 (15)	5336 (13)	825 (10)	60 (7)
C(31)	1339 (17)	5960 (13)	877 (9)	56 (7)
C(32)	−3766 (15)	5798 (12)	1492 (10)	55 (7)
C(33)	−4466 (17)	7085 (13)	1370 (12)	73 (8)
C(34)	−3546 (21)	7728 (16)	1174 (14)	97 (11)
C(35)	−1987 (18)	7215 (13)	1049 (12)	69 (8)

[a] Equivalent isotropic U defined as one-third of the trace of the orthogonalized U_{ij} tensor.

were heated in the absence of light and found by EPR to also give rhenium carbonyl semiquinone products. This result strongly suggests that the $Re(CO)_5$ radical can be formed thermally as well as photochemically in the presence of quinone. Extended irradiation or reflux of these solutions eventually gave $Re(DBCat)_3$ and $Re(Cl_4Cat)_3$, linking initial formation of the $Re(CO)_4(SQ)$ species to formation of the $Re(Cat)_3$ complexes. The progressive development of the EPR spectrum of $Re(Cl_4Cat)_3$ from that of $Re(CO)_4(Cl_4SQ)$ is shown in Figure 1. In the case of the semiquinone complex, spin density is concentrated on the paramagnetic ligand giving a spectrum centered about a $\langle g \rangle$ value of 2.0022 with rhenium hyperfine coupling (^{185}Re, ^{187}Re $I = {}^5/_2$) of 35.1 G. The tris(catecholate)rhenium(VI) complex with a d^1 metal ion shows strong, field-dependent metal coupling ranging from 350 to 600 G at the high-field region of the spectrum.[9] While $Re(Cl_4Cat)_3$ can also be formed photochemically, carbon–chlorine bond insertion is a more significant side reaction under these conditions than when the reaction is carried out thermally. The presence of $ReCl(CO)_5$ has been established from FTIR spectra recorded on photolyzed solutions of tetrachloro-1,2-benzoquinone and dirhenium decacarbonyl.[10] Nucleophilic metal carbonyls have been observed to react with the C–Cl bonds of tetrachlorobenzoquinone in previous studies.[11]

These results point to the existence of both thermal and photochemical pathways to the formation of metal semiquinone and catecholate complexes from metal carbonyls. The reaction between $Re_2(CO)_{10}$ and 9,10-phenanthrenequinone carried out photochemically in a toluene–dichloromethane solution produced an air-stabile, maroon product that is diamagnetic in the solid state and shows infrared carbonyl stretching vibrations. Crystallographic characterization of the reaction product has shown it to be $Re_2(CO)_7(PhenSQ)_2$. This complex reacts thermally with 3,5-di-*tert*-butyl-1,2-benzoquinone to give $Re(DBCat)_3$ (eq 3). It fails to react further with 9,10-phenanthrenequinone under either thermal or photochemical conditions to give $Re(PhenCat)_3$, however.

Structural Features of $Re_2(CO)_7(PhenSQ)_2$. The crystalline product obtained from the photochemical reaction between $Re_2(CO)_{10}$ and 9,10-phenanthrenequinone, $Re_2(CO)_7(PhenSQ)_2$,

(10) Abel, E. W.; Hargreaves, G. B.; Wilkinson, G. *J. Chem. Soc.* **1958**, 3149.
(11) Buchanan, R. M.; Fitzgerald, B. J.; Pierpont, C. G. *Inorg. Chem.* **1979**, *18*, 3439.

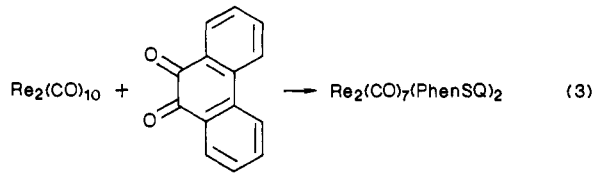

$Re_2(CO)_7(PhenSQ)_2$ + DBBQ → $Re(DBCat)_3$

consists of $Re(CO)_4(PhenSQ)$ and $Re(CO)_3(PhenSQ)$ units linked by the semiquinone oxygen atom of the $Re(CO)_4(PhenSQ)$ unit. Oxygen O8 of this ligand bridges the two metal ions, occupying the sixth coordination site of the $Re(CO)_3(PhenSQ)$ unit. Figures 2 and 3 contain views of the complex molecule, and selected bond lengths and angles of the structure are listed in Table III. Figure 3 shows the pyramidal geometry about O8, and the C8–O8 bond length of 1.347 (16) Å is typical of single carbon–oxygen bonds found for catecholate ligands. These features indicate a significantly more localized electronic structure for this semiquinone ligand relative to chelated semiquinones and to the second ligand of this molecule.[7] The second C–O length of this ligand (1.274 (13) Å) and the two carbonyl lengths of the second semiquinone ligand, 1.276 (18) and 1.287 (14) Å, agree well with values found typically for semiquinones. Rhenium–oxygen lengths show that the bridge is unsymmetrical, with the Re1–O8 length within the chelate ring shorter by 0.1 Å than the outer orbital bond to Re2. All Re–O lengths of the structure are significantly longer than values in the 1.93–1.94 Å range observed for the $Re(DBCat)_3$ and $Re(Cl_4Cat)_3$ complexes.[9] Rhenium–carbon lengths to the carbonyl ligands show expected patterns where lengths to the $Re(CO)_3$ metal, Re2, are shorter than values to the $Re(CO)_4$ metal, and Re–C lengths trans to oxygen atoms are shorter than values trans to other carbonyl bonds. The Re1–Re2 separation of 3.910 (2) Å precludes any strong, direct metal–metal interaction.

The observed diamagnetism of the complex in the solid state requires a strong spin–spin coupling interaction between semiquinone ligands. Octahedra are in a staggered orientation for the two metals, with planes of the two phenanthrenesemiquinones paired in the parallel arrangement shown in Figures 2 and 3. The dihedral angle between ligand planes is 16.1°, and the shortest interatomic contacts between atoms of the two semiquinones, listed in Table III, occur for atoms of the carbonyl regions. The C8–C22 and O8–O11 contacts are shortest with values of 2.69 Å and the O8–Re2–O11 angle is the most contracted octahedral bond angle of the structure with a value of 74.5 (3)°. A similar interaction is found for $Mo_2O_5(PhenSQ)_2$ which is also diamagnetic in the solid state.[12] In this case the dihedral angle between phenanthrenesemiquinone ligand planes was 19.3° and closest interatomic contacts between ligands also occurred for the carbonyl atoms with values also in the 2.6–2.8-Å range.

Spectroscopic Properties of $Re_2(CO)_7(PhenSQ)_2$. Infrared spectra were recorded on $Re_2(CO)_7(PhenSQ)_2$ as solid state KBr pellets and in CH_2Cl_2 and THF solutions. The solid-state spectrum shows six bands in the metal–carbonyl region at 2113, 2015, 1985, 1933, 1914, and 1894 cm^{-1}. The lower energy carbonyl bands approach the region associated with semibridging carbonyl ligands. The Re–C–O bond angles of the structure are all normal, however, and these bands are likely due to the strongly bonded carbonyls of the $Re(CO)_3$ fragment. Solution spectra recorded in both solvents showed only slight shifts in band positions and were quite similar to solid spectra, suggesting that dissociation of the binuclear complex does not occur. This is of interest because in similar solutions the complex exhibits an EPR spectrum. The spectrum, shown in Figure 4, is similar to that of $Re(CO)_4(Cl_4SQ)$, and it consists of six lines due to the $I = {}^5/_2$ ^{185}Re and ^{187}Re nucleii, centered about a $\langle g \rangle$ value of 2.0017, with rhenium hyperfine coupling of 17.6 G (toluene). Examination of the spectral lines at high resolution over the temperature range from +35 to −90 °C has failed to indicate the presence of two superimposed spectra. As the temperature of the solution is decreased, hyperfine lines

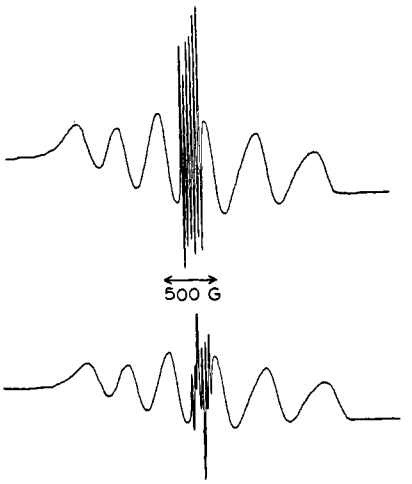

Figure 1. EPR spectral changes that occur when a toluene solution containing $Re_2(CO)_{10}$ and tetrachloro-1,2-benzoquinone is heated at reflux. The upper spectrum recorded after 4 h shows the weakly coupled spectrum of $Re^{I}(CO)_4(Cl_4SQ)$ superimposed on the strongly coupled spectrum of $Re^{VI}(Cl_4Cat)_3$. After 5 h (lower spectrum) much of the $Re(CO)_4(Cl_4SQ)$ has been converted to $Re(Cl_4Cat)_3$.

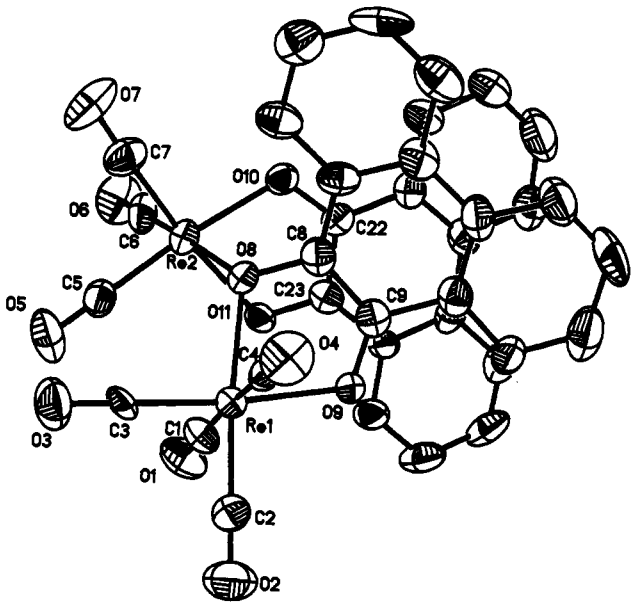

Figure 2. View of $Re_2(CO)_7(PhenSQ)_2$ showing the pairing interaction between semiquinone ligands.

due to the rhenium nucleii coalesce to give two lines separated by 64 G at −80 °C.

Wan has reported the formation of $Re(CO)_4(PhenSQ)$ by procedures similar to those used in our investigation and has indicated that this complex shows rhenium hyperfine coupling of 22.2 G (benzene).[5f] We can therefore rule out the presence of $Re(CO)_4(PhenSQ)$ in solution and conclude that pairing of the semiquinone ligands is broken up by rotation about the Re2–O8 bond to give an associated bis(semiquinone) complex without

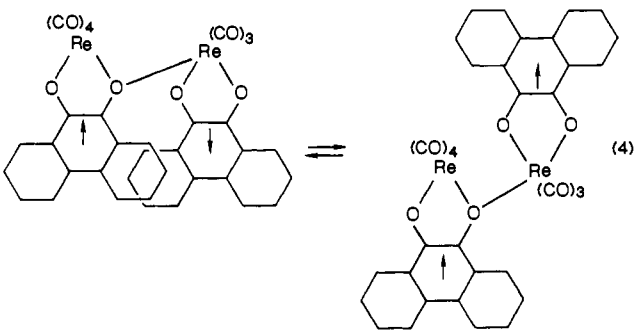

(12) Pierpont, C. G.; Buchanan, R. M. *J. Am. Chem. Soc.* **1975**, *97*, 6450.

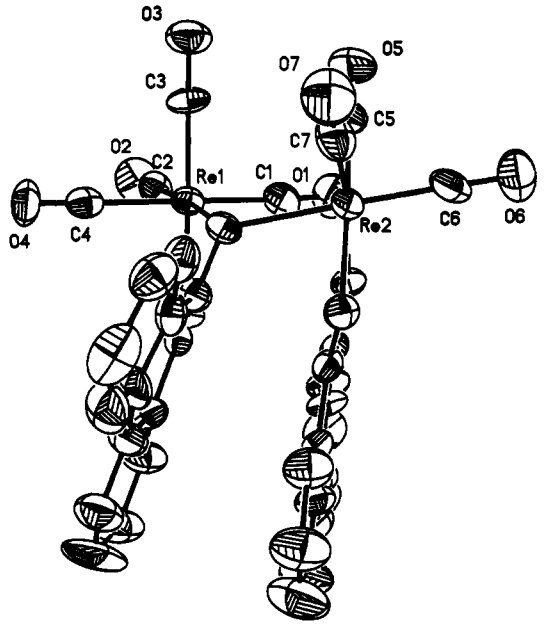

Figure 3. View of $Re_2(CO)_7(PhenSQ)_2$ showing the O8 bridge between metal atoms.

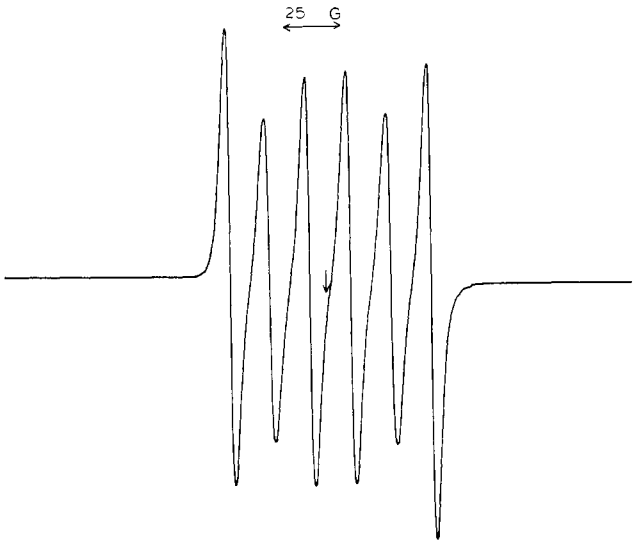

Figure 4. View showing the EPR spectrum of $Re_2(CO)_7(PhenSQ)_2$ recorded in toluene at 298 K. The spectrum is centered about a $\langle g \rangle$ value of 2.0017 with Re hyperfine coupling of 17.6 G. The DPPH standard value is denoted by the arrow.

coupling between paramagnetic ligands (eq 4). In this case spectral parameters for the two nonequivalent semiquinones are either the same or are time-averaged by rapid carbonyl ligand exchange between the two metal atoms.

Electrochemistry on $Re_2(CO)_7(PhenSQ)_2$. Solutions prepared with $Re_2(CO)_7(PhenSQ)_2$ in dichloromethane were studied by using cyclic voltammetry and constant potential coulometry. The complex undergoes two-electron reduction reversibly at −0.68 V (vs Fc/Fc^+), with a separation of 110 mV between cathodic and anodic peaks at a scan rate of 100 mV/s. At more rapid scan rates the cathodic peak remains unchanged, but at a scan rate of 500 mV/s the anodic peak is split to give two one-electron oxidations differing in potential by roughly 80 mV. Coulometric reduction gives a green EPR silent product which undergoes air oxidation to give the original, neutral complex. The complex also undergoes reversible two-electron oxidation at +0.26 V with a peak separation of 65 mV at 100 mV/s. At scan rates of over 200 mV/s the oxidation process can be resolved into two reversible one-electron couples at +0.14 V (ΔE = 42 mV) and +0.25 V (ΔE = 70 mV). Coulometric oxidation of the neutral complex gave a dark green EPR silent product. While detailed studies have not been carried out, given the reversibility and the potentials of the redox processes, it is likely that both the reduction and oxidation reactions occur at the quinone ligands.

Table III. Selected Bond Lengths and Angles for $Re_2(CO)_7(PhenSQ)_2$

	Bond Lengths (Å)		
Re1–O8	2.218 (7)	Re2–O8	2.310 (9)
Re1–O9	2.135 (8)	Re2–O10	2.117 (7)
Re1–C1	1.983 (14)	Re2–O11	2.134 (9)
Re1–C2	1.901 (12)	Re2–C5	1.897 (11)
Re1–C3	1.896 (13)	Re2–C6	1.851 (17)
Re1–C4	2.036 (15)	Re2–C7	1.891 (17)
	Phenanthrenequinone **1**		
O8–C8	1.347 (16)	C10–C11	1.428 (19)
O9–C9	1.274 (13)	C11–C12	1.434 (25)
C8–C9	1.420 (22)	C12–C13	1.407 (21)
C9–C10	1.457 (19)	C13–C8	1.419 (17)
	Phenanthrenequinone **2**		
O10–C22	1.276 (18)	C24–C25	1.419 (17)
O11–C23	1.287 (14)	C25–C26	1.469 (18)
C22–C23	1.456 (16)	C26–C27	1.415 (22)
C23–C24	1.446 (21)	C27–C22	1.459 (17)
	Carbonyl Ligands		
C1–O1	1.140 (18)	C5–O5	1.143 (14)
C2–O2	1.137 (15)	C6–O6	1.170 (20)
C3–O3	1.163 (16)	C7–O7	1.156 (22)
C4–O4	1.116 (19)		
	Angles (deg)		
Re1–C1–O1	174.8 (9)	Re1–O8–C8	107.9 (8)
Re1–C2–O2	179.1 (11)	Re1–O9–C9	112.1 (9)
Re1–C3–O3	179.8 (14)	Re1–O8–Re2	119.4 (3)
Re1–O8–C8	108.0 (8)	Re2–O8–C8	117.3 (6)
Re1–C4–O4	177.4 (10)	Re2–O10–C22	114.1 (6)
Re2–C5–O5	177.1 (13)	Re2–O11–C23	115.2 (7)
Re2–C6–O6	178.8 (13)	O8–Re1–O9	75.1 (3)
Re2–C7–O7	176.6 (11)	O10–Re2–O11	75.6 (3)
C1–Re1–C2	86.1 (5)	C5–Re2–C6	85.6 (6)
C1–Re1–C3	89.9 (6)	C5–Re2–C7	86.6 (6)
C1–Re1–C4	176.3 (5)	C5–Re2–O8	93.2 (5)
C1–Re1–O8	96.5 (4)	C5–Re2–O10	174.9 (5)
C1–Re1–O9	93.6 (4)	C5–Re2–O11	99.7 (5)
C2–Re1–C3	85.8 (6)	C6–Re2–C7	83.6 (7)
C2–Re1–C4	90.2 (5)	C6–Re2–O8	176.4 (5)
C2–Re1–O8	174.6 (5)	C6–Re2–O10	97.5 (4)
C2–Re1–O9	100.0 (5)	C6–Re2–O11	102.4 (5)
C3–Re1–C4	90.3 (6)	C7–Re2–O8	99.7 (5)
C3–Re1–O8	98.9 (4)	C7–Re2–O10	97.9 (5)
C3–Re1–O9	173.4 (4)	C7–Re2–O11	171.5 (5)
C4–Re1–O8	87.2 (4)	O8–Re2–O10	83.5 (3)
C4–Re1–O9	86.5 (4)	O8–Re2–O11	74.5 (3)
	Dihedral Angle (deg)		
	PhenSQ1–PhenSQ2	16.1	
	PhenSQ1–PhenSQ2 Contacts Less Than 3.1 Å		
C8–C22	2.69	C8–C23	2.88
O8–O11	2.69	O8–O10	2.95
C8–O10	2.84	O8–C23	3.06
C9–C23	2.86	O11–C8	3.09

Discussion

Metal–carbonyl complexes have been found to be useful precursors to metal–quinone complexes. The results of this study show that both thermal and photochemical routes exist for these reactions. The thermal reaction is preferred for $Re(Cl_4Cat)_3$ due to side reactions involving metal insertion into ring C–Cl bonds; the photochemical procedure is the most efficient route to $Re(DBCat)_3$. Both reactions may proceed by formation of the reactive $Re(CO)_5$ radical. However, under thermal conditions where homolytic cleavage of $Re_2(CO)_{10}$ fails to occur, the initial reaction must involve the unsaturated $Re_2(CO)_9$ species formed by carbonyl displacement. Addition of benzoquinone, followed by electron transfer to the quinone and dissociation, would produce both $Re(CO)_5$ and $Re(SQ)(CO)_4$ (eq 5). The addition of

$$Re_2(CO)_9 + BQ \rightarrow Re_2(CO)_9(BQ) \rightarrow Re(CO)_5 + Re(SQ)(CO)_4 \quad (5)$$

phosphine ligands to thermally generated $Re_2(CO)_9$ has been observed to occur reversibly and without Re–Re bond cleavage. Reduction of the quinone of $Re_2(CO)_9(BQ)$ would occur with oxidation of the metal–metal bond, leading to dissociation. Consequently, reactions, thermal or photochemical, that lead to formation of $Re(SQ)(CO)_4$ do not necessarily proceed by initial formation of $Re(CO)_5$ radical. Photoexcitation of the quinone could potentially contribute to the reaction, but we find no evidence for this in the Re–quinone systems. Carbonyl displacement from $Re(SQ)(CO)_4$ to give unsaturated $Re(SQ)(CO)_3$ appears to occur thermally, and possibly also photochemically, in the process of adding the second quinone ligand. However, even in the presence of excess 9,10-phenanthrenequinone, $Re(PhenSQ)(CO)_3$ prefers to bond with the semiquinone oxygen of $Re(PhenSQ)(CO)_4$ rather than to add an additional quinone ligand. Quinone addition to $Re_2(CO)_7(PhenSQ)_2$ occurrs oxidatively with carbonyl ligand displacement to give $Re^{VI}(Cat)_3$ when tetrachloro-1,2-benzoquinone or 3,5-di-*tert*-butyl-1,2-benzoquinone is used. This is perhaps expected, but the absence of a reaction with additional 9,10-phenanthrenequinone is surprising. The reduction potential of phenanthrenequinone is slightly more negative than that of di-*tert*-butylbenzoquinone by 0.07 V, but this is the only obvious difference between the quinones used in this study.[13]

Reactions carried out with $Cr(CO)_6$ have also shown that both thermal and photochemical pathways exist. Both $Cr(Cl_4SQ)_3$ and $Cr(DBSQ)_3$ can be formed by reactions of both types, while $Cr(PhenSQ)_3$ can only be formed by a thermal reaction.[14] In contrast, the reaction between $Mo(CO)_6$ and 9,10-phenanthrenequinone occurrs photochemically,[12] while reactions with tetrachlorobenzoquinone and 3,5-di-*tert*-butylbenzoquinone are thermal.[15,16] While both types of reactions exist as options for the metal carbonyl–quinone systems, it remains unclear as to which procedure is best for a particular metal–quinone combination.

Acknowledgment. This research was supported by the National Science Foundation under Grants CHE 85-03222 and CHE 84-12182 (X-ray instrumentation).

Supplementary Material Available: Tables containing anisotropic thermal parameters and a complete list of bond distances and angles for $Re_2(CO)_7(PhenSQ)_2$ (6 pages); listing of observed and calculated structure factors (42 pages). Ordering information is given on any current masthead page.

(13) Bradbury, J. R.; Schultz, F. A. *Inorg. Chem.* **1986**, *25*, 4416.
(14) (a) Pierpont, C. G.; Downs, H. H. *J. Am. Chem. Soc.* **1976**, *98*, 4834. (b) Vlcek, A., Jr. *Inorg. Chem.* **1986**, *25*, 522.
(15) Pierpont, C. G.; Downs, H. H. *J. Am. Chem. Soc.* **1975**, *97*, 2123.
(16) Cass, M. E.; Pierpont, C. G. *Inorg. Chem.* **1986**, *25*, 122.

Nitroethylene Yields *N,N*-Dihydroxyiminium–Methylium Dication in Trifluoromethanesulfonic Acid. Dications Stabilized by Y Delocalization

Tomohiko Ohwada, Akiko Itai, Toshiharu Ohta, and Koichi Shudo*

Contribution from the Faculty of Pharmaceutical Sciences, University of Tokyo, 7-3-1, Hongo, Bunkyo-ku, Tokyo 113, Japan. *Received November 25, 1986. Revised Manuscript Received June 1, 1987*

Abstract: The results of acid-catalyzed reactions and NMR spectroscopic investigations demonstrate the formation from nitroethylene in trifluoromethanesulfonic acid of a novel dication, *N,N*-dihydroxyiminium–methylium dication, which lacks the stabilization of an adjacent aromatic nucleus. The formation of this simple acyclic dication can be ascribed to an intrinsic stabilization, probably by Y delocalization, owing to the six delocalized electrons (two π-electrons of the olefinic bond and four electrons of lone pairs of two hydroxyl groups) in the whole system: this system is isoelectronic with a guanidinium ion. Ab initio calculations confirmed the presence of stabilization effects arising from delocalization of six π-electrons in the dication.

Diprotonation of nitro groups in a strong acid, trifluoromethanesulfonic acid (TFSA), is a novel phenomenon, which was discovered for the first time in nitronaphthalenes.[1] Recently, we investigated the protonation of nitro groups of β-nitrostyrenes. On the basis of the value of the cryoscopic constant of TFSA, it was concluded that O,O-diprotonated β-nitrostyrenes (*N,N*-dihydroxyiminium–benzylium dications **1**) are formed in TFSA (Figure 1).[2] A further study described the reaction of the dications **1** as novel reactive electrophiles.[3] The dication **1** is quite stable for hours under suitable conditions, even at 0 °C. We have attributed the very great stability of these dipositively charged species to the effective stabilization of the cation center (C_2) by conjugation with the aromatic ring. In this paper, however, we present the surprising result that a simple nitro olefin (nitroethylene for example) is also diprotonated in TFSA to form the *N,N*-dihydroxyiminium–carbenium dication. This suggests the existence of intrinsic stabilization of the dication.

(1) Ohta, T.; Shudo, K.; Okamoto, T. *Tetrahedron Lett.* **1984**, 325.
(2) Ohwada, T.; Ohta, T.; Shudo, K. *J. Am. Chem. Soc.* **1986**, *108*, 3029.
(3) Ohwada, T.; Ohta, T.; Shudo, K. *Tetrahedron* **1987**, *43*, 297.

Results and Discussion

Acid-Catalyzed Reactions of Nitro Olefins with Benzene. In the reaction with benzene, the dication **1** gave diphenylacetophenone oxime (**3**) in quantitative yield (Figure 2).[3] The fact that the reaction is catalyzed by more than 2 equiv of the acid supports the conclusion that the electrophile is the *N,N*-dihydroxyiminium–benzylium dication. Thus, the acid-catalyzed reaction of nitroethylene was investigated.

In the presence of TFSA (10 equiv with respect to the nitro olefin), nitroethylene (**4**) reacts with benzene to afford deoxybenzoin oxime (**5**) in quantitative yield (96%). The starting material disappears rapidly and the reaction is clean. One equivalent of TFSA did not catalyze the reaction even at room temperature. If a monoprotonated nitroethylene had sufficient reactivity, the product should have been obtained even when 1 equiv of TFSA was used. The reaction of **4** is in exactly the same

0002-7863/87/1509-7036$01.50/0